

01 Jan 1991

## An Optoelectronic Adaptive Resonance Unit

Donald C. Wunsch

Missouri University of Science and Technology, [dwunsch@mst.edu](mailto:dwunsch@mst.edu)

T. P. Caudell

R. A. Falk

C. David Capps

Follow this and additional works at: [https://scholarsmine.mst.edu/ele\\_comeng\\_facwork](https://scholarsmine.mst.edu/ele_comeng_facwork)

 Part of the [Electrical and Computer Engineering Commons](#)

---

### Recommended Citation

D. C. Wunsch et al., "An Optoelectronic Adaptive Resonance Unit," *Proceedings of the International Joint Conference on Neural Networks, 1991., IJCNN-91-Seattle*, Institute of Electrical and Electronics Engineers (IEEE), Jan 1991.

The definitive version is available at <https://doi.org/10.1109/IJCNN.1991.155236>

This Article - Conference proceedings is brought to you for free and open access by Scholars' Mine. It has been accepted for inclusion in Electrical and Computer Engineering Faculty Research & Creative Works by an authorized administrator of Scholars' Mine. This work is protected by U. S. Copyright Law. Unauthorized use including reproduction for redistribution requires the permission of the copyright holder. For more information, please contact [scholarsmine@mst.edu](mailto:scholarsmine@mst.edu).

# An Optoelectronic Adaptive Resonance Unit

Donald C. Wunsch II, Thomas P. Caudell, C. David Capps, and R. Aaron Falk

The Boeing Company  
P.O. Box 24346, MS 6R-08  
Seattle, WA 98124-0346  
dwunsch@atc.boeing.com

## Abstract

Adaptive resonance theory (ART) is an outgrowth of years of work by Stephen Grossberg and Gail Carpenter.<sup>1,2</sup> However, hardware implementation is just beginning to be addressed. We demonstrate a hardware implementation of the ART1 neural network architecture. Recently, a similar system based on optical hardware was described.<sup>3</sup> The device, however, used a fixed hologram, and was therefore not capable of learning. Also recently, an electronic implementation of ART was designed. Although this device would probably be successful if implemented, it requires time multiplexing of the inner product calculations required, which leaves open the possibility of achieving a higher performance in an optical implementation.<sup>4</sup> This paper addresses an innovation that allows parallel execution of the most computationally intensive parts of the network model by using optical hardware. We begin with a very brief review of ART1 as an algorithm, then explain the hardware and show experimental results.

## ART1 as an algorithm

ART1 has been described in algorithmic form elsewhere<sup>5</sup>, so we only make a brief review here. Consider a new  $n$ -element binary input vector to be called  $P$ . We wish to assign the vector to a category, such as category 1, category 2, etc. Each category will have a template associated with it. The unit will compare the input to these patterns to decide how to classify it. We will index the templates and refer to them as the  $T_i$ , where  $i$  is the index number. All of the vectors have  $n$  elements. With these definitions in mind, the full ART1 algorithm is given in the flowchart of Figure 1 below.<sup>12</sup> A key thing to notice is the test

$$\frac{T_i \cdot I}{I \cdot I} < \rho, \quad (1)$$

which determines the level of discrimination, coarse or fine, used in grouping. The parameter  $\rho$  is called the vigilance threshold. The other key point is that several inner product and norm calculations are required. These inner products are mathematically equivalent to correlations that can be performed optically.

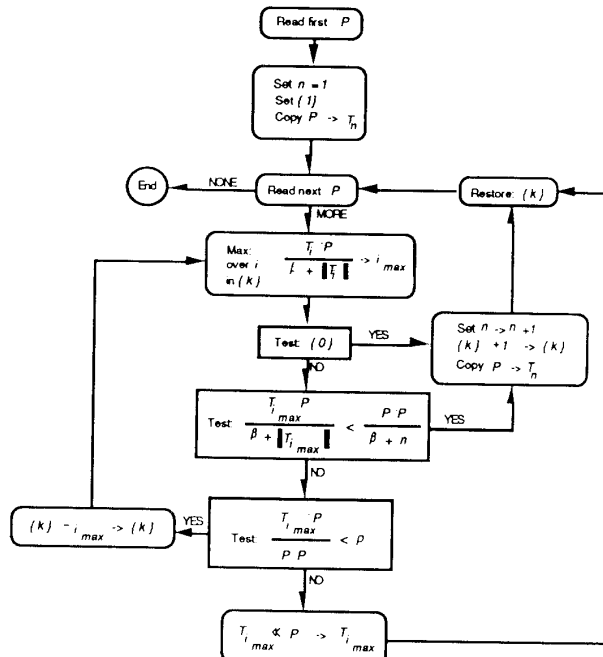


Figure 1. The ART1 algorithm.<sup>13</sup>

### The optical hardware: a Van der Lugt correlator

The optoelectronic ART1 unit is a novel application of an old device. This device--the 4-f or Van der Lugt correlator--has historically been used as a fast pattern classifier. Usually the correlation operation is employed as a matched filter, so that a maximum correlation peak corresponds to a well-matched pattern. The device described here also uses the large peaks, but takes specific advantage of the fact that a zero-shift correlation is mathematically equivalent to a two-dimensional inner product, which is an essential computation for an ART unit. This device measures relative values of strong and weak correlation peaks and interprets these as inner products. Therefore, for this application of the 4-f correlator, greater measurement accuracy is required, and more of the output gets used.

The device (shown in Figure 2) consists of two lenses, a polarizer, two spatial light modulators (SLMs), a laser (not shown), a charge-coupled-device (CCD) camera, and a computer. This experimental setup has demonstrated several kinds of optical computing operations.<sup>5-8</sup> All electronic calculations are done by a DEC MicroVAX, which processes the CCD camera output via a frame grabber and controls the SLMs. The lenses both have focal length  $f$ , and all components are placed at a distance  $f$  from their neighbors. The light, traveling from left to right, comes from a helium-neon laser (not shown) emitting at 632.8 nm. This type of optical correlator was invented by Anthony Van der Lugt<sup>5</sup> in 1964.

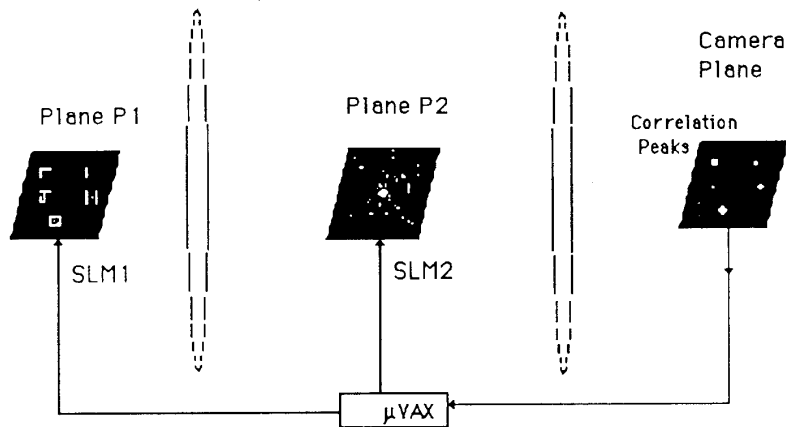


Figure 2. The 4-f correlator can do the most demanding computations of an ART1 unit.

The device is based on the concept of matched filtering. The reason for using matched filters is to be able to determine which of several stored patterns most closely matches the input pattern. To do this, a bank of templates are transformed into filters in the frequency domain by the first lens. The input is numerically Fourier transformed, placed on an SLM2, and optically multiplied by each filter. Then a second Fourier transform is taken by the second lens. The result gives the cross-correlation of the input pattern and the templates. The maximum output possible occurs when the input matches a template. It is also significant that, in the classical theory, the filter encoded in the frequency domain is the complex conjugates of the Fourier transforms of the input pattern in the spatial domain. It is now popular to deviate from this design by making a phase-only filter (POF), which will be discussed later.

Now let us examine how the optical correlator implements the matched filter. Plane P1 contains the amplitude-encoded pattern  $f(x,y)$ , which is displayed on the first spatial light modulator. (Ultimately we will be placing a whole set of templates here, but we will first discuss the case of a single pattern.) This pattern can be changed by the computer. The pattern  $f(x,y)$  can be thought of as an input to the correlator or as a template. In this application we use it as a template. Plane P2, containing the second SLM, is the location of the conjugate of the Fourier transform of the pattern to be correlated with  $f(x,y)$ . Let us refer to this transform as  $G^*(u, v)$ , the conjugated Fourier transform of  $g(x,y)$ . Note that the SLMs are a focal length to either side of the first lens. According to the classical theory<sup>8</sup>, this means the pattern  $f(x,y)$  is Fourier transformed and multiplied by  $G^*(u,v)$ . The multiplied transforms are again transformed by the second lens. This implies, by the correlation theorem, that the pattern seen on the output contains the correlation of  $f$  and  $g$ . This is recorded by the CCD camera and fed into the computer.

The expression for the output of the correlator can be expressed in terms of the correlation operator  $\star$  and of  $\mathcal{F}[\cdot]$ , the 2-D Fourier transform operator, as follows:

$$\mathcal{F}[A_0 \mathcal{F}(u, v) G^*(u, v)] = A_0 \int_{-\infty}^{\infty} \int_{-\infty}^{\infty} G^*(u, v) \cdot \left[ \int_{-\infty}^{\infty} \int_{-\infty}^{\infty} f(x, y) e^{-j\frac{2\pi}{\lambda f}(xu + yv)} dx dy \right] e^{-j\frac{2\pi}{\lambda f}(ux_2 + vy_2)} du dv \quad (2)$$

$$= A_1 \int_{-\infty}^{\infty} \int_{-\infty}^{\infty} f(x, y) \cdot \left[ \int_{-\infty}^{\infty} \int_{-\infty}^{\infty} G^*(u, v) e^{j\frac{2\pi}{\lambda f}(u(-x-x_2) + v(-y-y_2))} du dv \right] dx dy \quad (3)$$

$$= A_2 \int_{-\infty}^{\infty} \int_{-\infty}^{\infty} f(x, y) \mathcal{F}[\mathcal{F}[g(x+x_2, y+y_2)]] dx dy \quad (4)$$

$$= A_2 f \star g, \text{ which is the desired correlation, except for a coordinate reversal.} \quad (5)$$

We have ignored the effects of the constants  $A_0$ ,  $A_1$ , and  $A_2$ . The center point of the correlation peak is proportional to the inner product of  $f$  and  $g$ , so the device can be used to measure the inner products given in the previous section.

It is possible to compute the correlation, and therefore the inner products, of multiple patterns simultaneously using this device, because the SLMs are small ( $2.5 \text{ cm}^2$ ) compared to the focal lengths of the lenses (38 cm). Thus, the paraxial approximation applies, and if multiple patterns are placed on SLM1, all of their Fourier transforms will be approximately centered on SLM2. This results in multiple correlation peaks on the output positioned in correspondence with the center location of the input patterns. This arrangement is especially convenient for an implementation of ART1. The patterns chosen for SLM1 are all the templates known at present, along with a copy of the input pattern. SLM2 contains the conjugate of the Fourier transform of the input pattern. The inner product of the input with itself and with all templates is thus calculated in a massively parallel fashion. However, it is important to point out that the pattern on SLM2 is not really the conjugated Fourier transform of the input, but rather the binary phase-only filter (BPOF) based on that transform. This has been shown to be preferable to the standard Fourier transform in several ways, explanation of which is beyond the scope of this work. The BPOF can be described by representing  $G(u, v)$  with the amplitude and phase information given separately:

$$G(u, v) = |G(u, v)| e^{j\phi[G(u, v)]} \quad (6)$$

The phase-only filter is given by:

$$G_{\phi}(u, v) = \frac{G(u, v)}{|G(u, v)|} = e^{(j\phi[G(u, v)])}, \quad (7)$$

which can be converted to a BPOF  $G_{B\phi}(u, v)$  by using a formula such as:

$$G_{B\phi}(u, v) = \begin{cases} 1 & \text{if } \text{Re}[G_{\phi}(u, v)] \geq 0 \\ -1 & \text{if } \text{Re}[G_{\phi}(u, v)] < 0. \end{cases} \quad (8)$$

### The optoelectronic ART experiments

The ART1 algorithm of Figure 1 was mapped onto the hardware and software of the 4-f correlator for testing. Validation of this design as a practical ART unit was provided by two key experiments: a demonstration of the reset mechanism and verification of the ability to write new templates as appropriate. To accomplish these, the

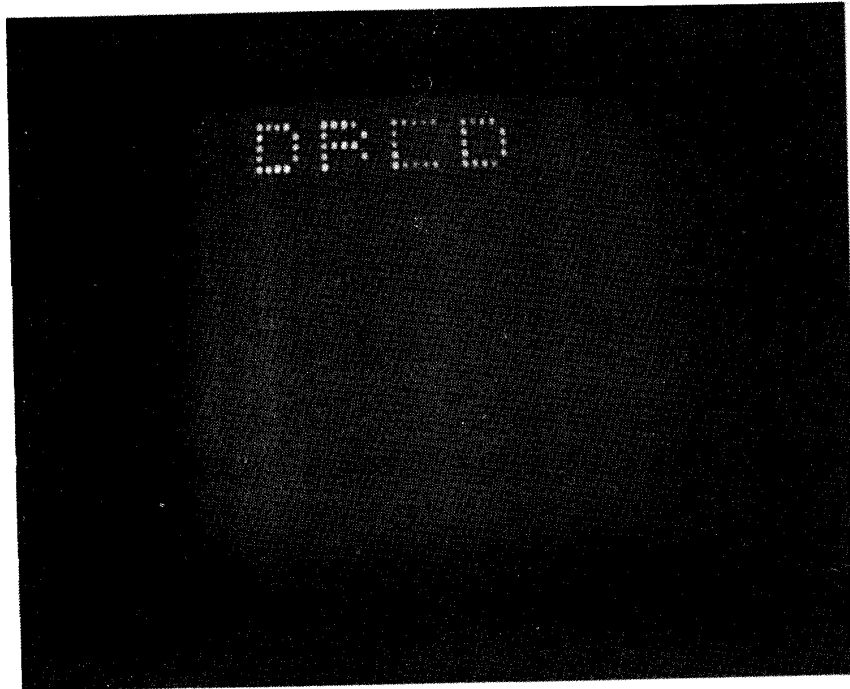


Figure 3. The optoelectronic ART1 unit, showing the correlator.

system had to be carefully calibrated to use peak heights as inner products, which is where the significant difference in the use of the optical correlator becomes apparent. When a Van der Lugt correlator is used simply as a matched filter bank, calibration is not even a concern, because the signal-to-noise ratio is high enough that the brightest peak will usually be the best correlation even without calibration. In contrast, for our ART1 implementation, the device is used to measure the inner products given in Figure 1, so greater accuracy, and thus calibration, is a matter of critical importance. The control code for the experiments begins by defining the data, parameters, and calibration

pattern(s) for the system. It then calls up the precomputed BPOF of the input image from a file. (In a practical implementation, the FFT and resulting filter would have to be calculated on the fly.) The user is prompted for the value of  $\rho$ , and the calibration routine begins. Then the SLMs are reinitialized and the first input pattern is presented. Subsequent input patterns are also written to SLM1, in a portion of the SLM reserved for the current input pattern. Then the BPOF of the new input pattern is loaded onto SLM2. The correlation values are read off the camera and are normalized according to the calibrations. Then the various test values for the ART1 algorithm are computed. The algorithm causes a reset or records a new or updated template on SLM1 as appropriate.

The experimental setup is shown in Figures 3 and 4. The capability to perform reset and to learn updated templates was demonstrated simultaneously by a number of learning examples with several different values of  $\rho$ . Some of the most significant of these are described below. One of the experiments with the  $\rho = 0$  case is shown in Figure 5. The output of the ART unit is displayed on the video monitor at the upper left. The pattern in the leftmost corner of the monitor is the current input pattern. All other patterns (in this case, there is only one) are the stored templates that have been learned up to the current time. Each time a template is updated by learning, the new

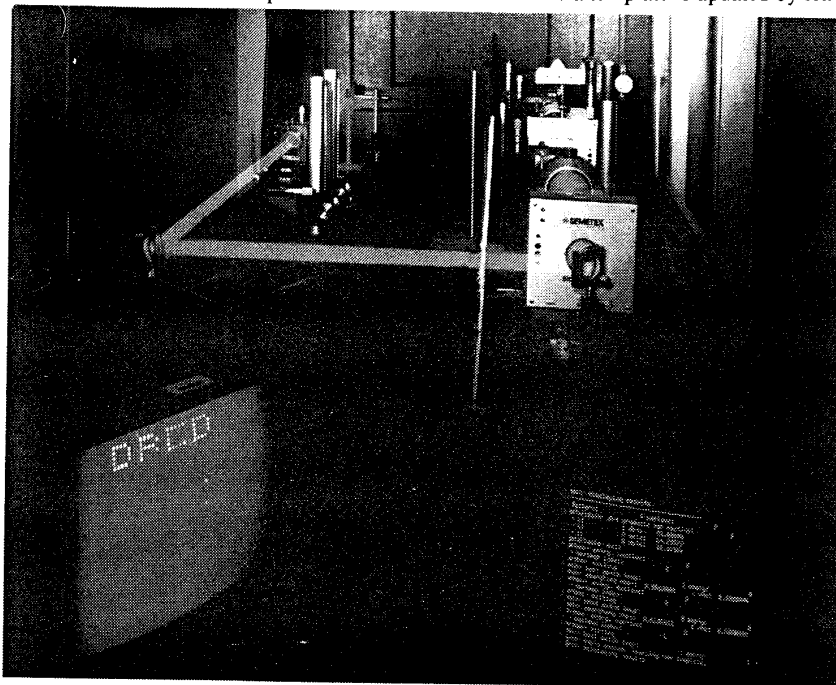


Figure 4. The optoelectronic ART1 unit, showing the full lab setup.

template is displayed on the monitor. Note that the correlation peaks for this example must ultimately become very weak, because the template is so small. Nevertheless, they are greater than zero, which is the value for  $\rho$ , so the  $\rho$  test from (1) never fails. These experiments verify the unit's ability to learn new templates. One of the

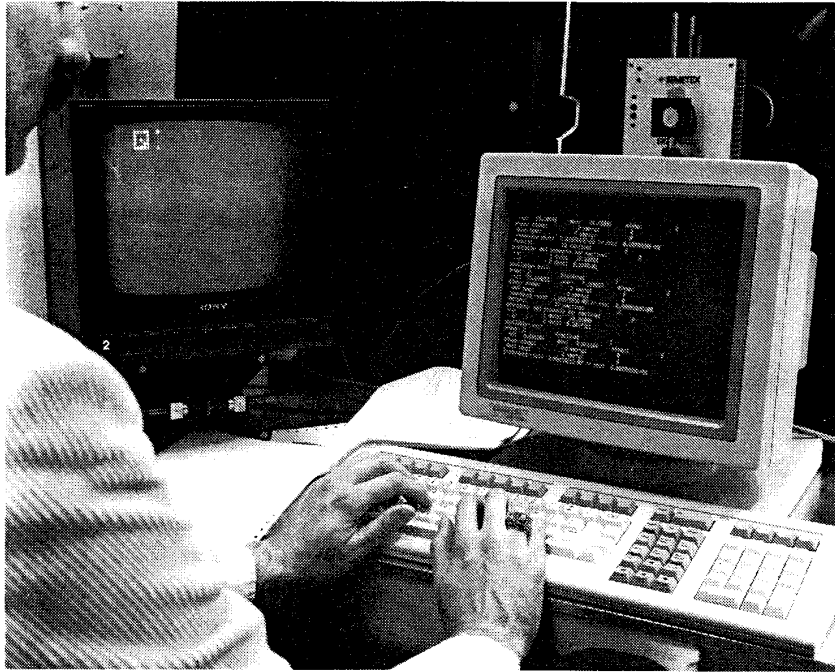


Figure 5. An experiment with the  $\rho = 0$  case.

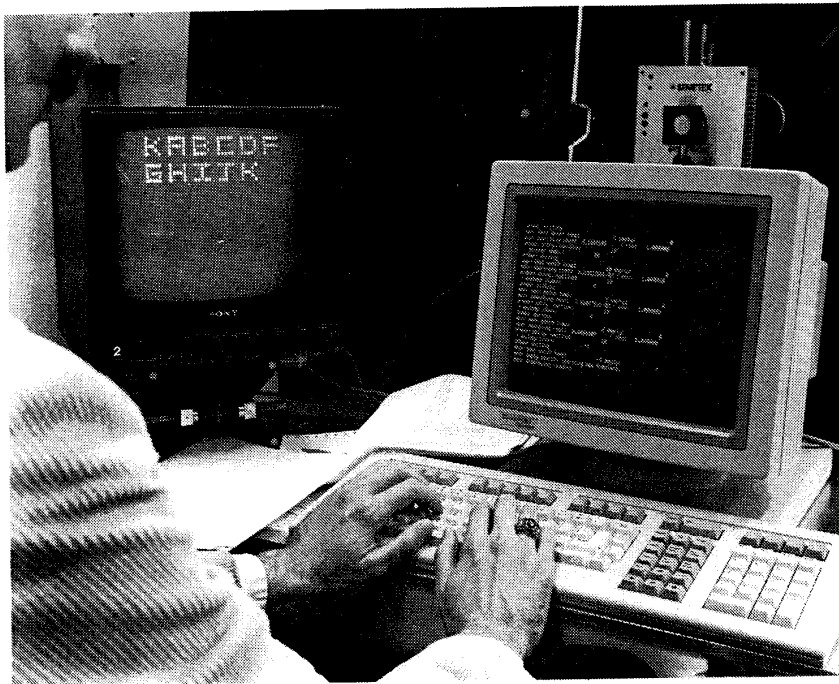


Figure 6. An experiment for the  $\rho = 1$  case.



experiments for the  $\rho = 1$  case is shown in Figure 6. This time, all distinct patterns create distinct templates. This is because the  $\rho = 1$  case requires perfect discrimination; even the smallest mismatch is not tolerated. Note that in this case the correlation peaks are relatively bright. However, if calibration has been done correctly, these values can never exceed one, so a new template must be generated. These experiments verify the unit's ability to reset in the event of a mismatch in the feedback expectancy portion of the ART1 algorithm. An experiment for an intermediate value of  $\rho$  is shown in Figure 7. As expected, this shows some patterns clustering together and some generating new templates, so we see the reset ability *and* the learning ability demonstrated. Note that different values of  $\rho$  provide different clusters and that the number of clusters generated increases with the value of  $\rho$ , as expected.

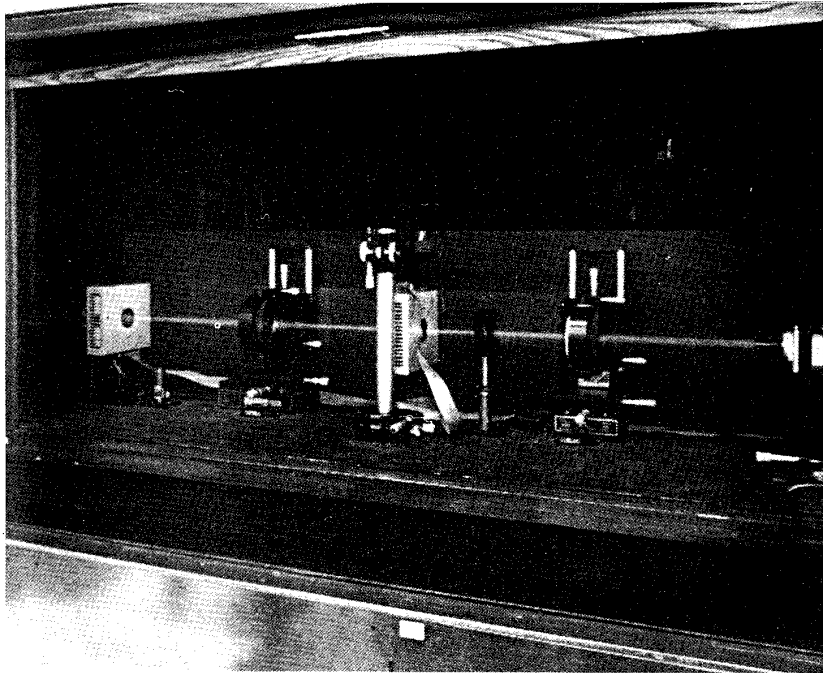


Figure 7. Experiment with an intermediate value of  $\rho$ .

## Conclusions

The important task of implementing neural network architectures such as ART is just beginning. We have shown a promising method for emulating an ART1 unit in optics. We have reviewed ART1 from an algorithmic point of view, which showed that inner products are a critical part of ART1. We then discussed its implementation, and showed some experimental results. The device works by performing the most computationally intensive parts of the algorithm in optical hardware, and thus offers a suitable marriage of the strengths of electronics and optics.

## References

1. Grossberg, Stephen, "Competitive learning: from interactive activation to adaptive resonance," *Cognitive Science*, 1987, No. 11, Cognitive Science Society, pp. 23-63.

2. Carpenter, Gail A., and Stephen Grossberg, "A massively parallel architecture for a self-organizing neural pattern recognition machine," *Computer Vision, Graphics, and Image Processing*, 1987, No. 37, Academic Press, Inc., pp. 54-115.
3. Caulfield, H. John, and David Armitage, "Adaptive resonance theory of optical pattern recognition," *Applied Optics*, 1 October 1989, Vol. 28, No. 19, Optical Society of America.
4. Rao, Arun, "VLSI implementation of neural classifiers," *Neural Computation*, No. 2, Massachusetts Institute of Technology, 1989, pp. 35-43.
5. Caudell, Thomas P. and Donald C. Wunsch II, "A hybrid optoelectronic ART1 neural processor", submitted to IJCNN-91-Seattle
6. Van der Lugt, A. B., "Signal detection by complex spatial filtering," *IEEE Transactions on Information Theory*, IT-10, No. 2, IEEE, 1964.
7. Horner, J. L., and P. D. Gianio, "Phase-only matched filtering," *Applied Optics*, V. 23, 1984, p. 812.
8. Goodman, Joseph W., *Introduction to Fourier Optics*, McGraw-Hill, San Francisco, 1968, pp. 141-184.
9. Capps, C. David, and S. G. Ferrier, "Toward practical real-time optical correlators," International Topical Meeting on Optical Computing, paper 10F3, Kobe, Japan, April 8-12, 1990.
10. Hestenes, David, "How the brain works: the next great scientific revolution," *Proceedings of the Third Workshop on Maximum Entropy and Bayesian Methods in Applied Statistics*, Univ. of Wyoming, August 1-4, 1983, Kluwer Academic Publishers.
11. Ryan, T. W., and C. L. Winter, "Variations on adaptive resonance," *Proceedings of the First International Conference on Neural Networks*, IEEE Catalog No. 87TH0191-7, pp. 767-776.
12. Healy, Michael J., "The elements of adaptive neural expert systems," *SPIE Vol. 1095, Applications of Artificial Intelligence VII*, SPIE, 1989, pp. 830-837.
13. Moore, Barbara, "ART1 and pattern clustering," *Proceedings of the 1988 Connectionist Summer School at Carnegie-Mellon University*, Touretzky and Hinton, eds., Morgan Kaufmann Inc., 1989.
14. Newman, David S. and Thomas P. Caudell, "Characterization of some learning properties of ART machines," *Neural Networks for Automatic Target Recognition*, poster paper, Wang Institute of Boston University, May 1990.